DOI: 10.1002/ejoc.200600520

# Full Structural Characterisation of the Lipooligosaccharide of a *Burkholderia pyrrocinia* Clinical Isolate

**Alba Silipo,[a] Antonio Molinaro,*[a] Daniela Comegna,[a] Luisa Sturiale,[b] Paola Cescutti,[c] Domenico Garozzo,[b] Rosa Lanzetta,[a] and Michelangelo Parrilli[a]**

**Keywords:** Lipopolysaccharides / Cystic fibrosis / Natural products

This paper deals with the full structural elucidation of the lipooligosaccharide from the Gram-negative bacterium *Burkholderia pyrrocinia*. *B. pyrrocinia* is one of the nine species included in the *Burkholderia cepacia* complex (BCC), a group of important opportunistic pathogens in patients with cystic fibrosis and chronic granulomatous disease. *B. pyrrocinia* strain BTS7, isolated from a patient with cystic fibrosis, was found to exclusively produce a lipooligosaccharide (LOS). This component of the external membrane plays a key role in the virulence of BCC bacteria and is required for resistance to antimicrobial compounds and for bacterial survival. Here we present, for the first time, a detailed study of the structure of the lipooligosaccharide (LOS) elucidated by means of compositional analysis, MALDI and ESI mass spectrometry and 2D NMR spectroscopy. The LOS of *B. pyrrocinia* was degraded by complete deacylation, dephosphorylation and reduction. The major oligosaccharide representing the carbohydrate backbone was isolated by size-exclusion chromatography and identified. The structural determination of molecules (such as the LOS of *B. pyrrocinia*) involved in the activation of the pro-inflammatory processes is the first step in the adoption of new therapeutic strategies against lung infections.



## Introduction

*Burkholderia cepacia* complex (BCC) is an important group of bacteria whose natural habitats are river sediments and soil around plants' roots. These microorganisms are also important opportunistic pathogens for cystic fibrosis (CF) patients since they can cause serious pulmonary infections associated with high mortality. In some CF patients BCC infection may lead to *B. cepacia* syndrome, a necrotizing pneumonia which culminates in rapid and fatal clinical deterioration.[1] In addition, evidence for patient-to-patient transmission and the characteristic multi-drug resistance of the members of the BCC has prompted the scientific community to study the virulence potential of these bacteria. The BCC comprises nine[2] different species which have all been isolated from CF patients; some of them are more virulent than others.

The pro-inflammatory potential of BCC strains is mainly due to their lipopolysaccharides (LPSs), whose toxicity involvement in septic shock is well known.[3–6] LPSs compose about 75% of the outer membrane of Gram-negative bacteria and are exposed towards the external environment. Lipopolysaccharides are heat-stable complex amphiphilic macromolecules that are indispensable for the growth and survival of Gram-negative bacteria.[3–6] They are built up according to a common structural architecture and are composed of a hydrophilic heteropolysaccharide (formed by a core oligosaccharide and an O-specific polysaccharide or O-chain) covalently linked to a lipophilic moiety termed lipid A, which is embedded in the outer leaflet and anchors these macromolecules to the membrane through electrostatic and hydrophobic interactions. LPSs without an O-chain are termed rough LPSs (R-LPSs) or lipooligosaccharides (LOSs). LOSs may occur either in wild strains, as in the case of *B. pyrrocinia*, or in laboratory strains possessing mutations in the genes encoding either the O-specific polysaccharide biosynthetic enzymes or proteins devoted to its transfer through the membrane. Lipid A possesses a rather conservative structure usually consisting of a β-(1→6)-glucosamine disaccharide backbone that is bis-phosphorylated and acylated with primary 3-hydroxy fatty acids at positions 2 and 3 of both GlcN residues; the hydroxy groups of the primary fatty acids can be further acylated by secondary acyl moieties.[4,6] In the core oligosaccharide, an inner and outer region are usually distinguished: the inner core,

[a] Dipartimento di Chimica Organica e Biochimica, Università degli studi di Napoli "Federico II",
Via Cinthia, 80126 Napoli, Italy
Fax: +39-081-674393
E-mail: molinaro@unina.it
[b] Istituto per la Chimica e la Tecnologia dei Materiali Polimerici, ICTMP – CNR,
Viale R. Margherita, 6, 95123 Catania, Italy
[c] Dipartimento di Biochimica, Biofisica e Chimica delle Macromolecole Università degli Studi di Trieste,
Via L. Giorgieri 1, 34127 Trieste, Italy

Supporting information for this article is available on the WWW under http://www.eurjoc.org or from the author.

  

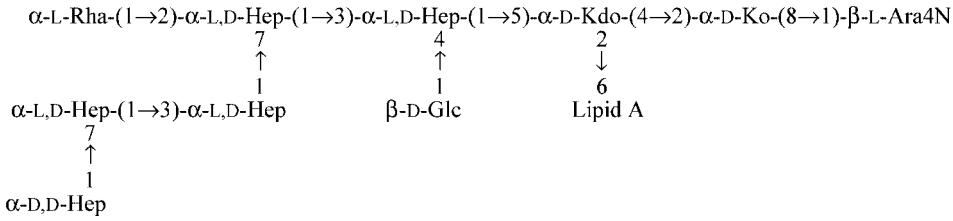


proximal to the lipid A, consists of typical monose residues like Kdo (3-deoxy-D-*manno*-oct-2-ulosonic acid) and heptoses. Kdo is the linker between the GlcN II of lipid A backbone and the core portion.[6] The outer core region is more variable and is usually composed of hexoses.

*B. pyrrocinia* strain BTS7 was isolated from a CF patient. A first microbiological characterisation of this strain classified it as belonging to the species *B. cepacia*.[7] However, the progress of the microbiological characterisation of this genus led us to identify it as *B. pyrrocinia* (Prof. P. Vandamme, personal communication). *B. pyrrocinia* strain BTS7 is a highly mucoid strain that produces abundant quantities of only one exopolysaccharide (Cepacian)[7] and has an outer membrane that is exclusively constituted by rough-type LPSs whose lipid A structure has been determined.[8] Here we present a detailed study of the structure of the LOS elucidated by means of compositional analysis, mass spectrometry and 2D NMR spectroscopy. The characterisation of the LOS of *B. pyrrocinia* involved in the activation of the pro-inflammatory process is a first important step toward the development of new therapeutic strategies against lung infections. The complete LOS structure is shown above.

## Results and Discussion

### Isolation and Compositional Analysis of LOS

The LOS (R-LPS) was obtained by phenol/chloroform/light petroleum extraction and lyophilized. The isolated LPS was a rough type (LOS), as suggested by the SDS-PAGE, which showed a run at the bottom of the gel; it was eventually purified by enzymatic hydrolysis with protease, DNAse and RNAse, followed by dialysis and Sephacryl HR-300 chromatography.

Monosaccharide analysis of the isolated LOS revealed the presence of L-Rha, D-GlcN, 4-amino-4-deoxy-L-arabinose (L-Ara4N), D-Glc, L-*glycero*-D-*manno*-heptose (L,D-Hep), D-*glycero*-D-*manno*-heptose (D,D-Hep), 3-deoxy-D-*manno*-oct-2-ulopyranosonic acid (D-Kdo) and D-*glycero*-D-*talo*-oct-2-ulopyranosonic acid (D-Ko). Methylation analysis revealed the presence of 3,4-substituted Hep, 2,7-substituted Hep, 3-substituted Hep, 7-substituted Hep, terminal L,D-Hep, terminal D,D-Hep, terminal D-Glc, terminal L-Rha, terminal L-Ara-4N, 6-substituted D-GlcN, 8-substituted D-Ko, 4,5-substituted D-Kdo and terminal D-Ko, all in pyranose rings.

Fatty acids analysis revealed the presence of (*R*)-3-hydroxyhexadecanoic acid [C16:0 (3-OH)] in an amide linkage and (*R*)-3-hydroxytetradecanoic acid [C14:0 (3-OH)] and tetradecanoic acid (C14:0) in an ester linkage. The primary structure of the core-lipid A region was determined by chemical analysis, mass spectrometry and NMR spectroscopy on intact and partially degraded LOS.

### Structural Characterisation of the Product OS

In order to determine the primary structure of the oligosaccharide portion from *B. pyrrocinia*, the LOS was fully deacylated, dephosphorylated and reduced, and the obtained oligosaccharide (OS) isolated by size-exclusion chromatography.

The compositional analysis of the isolated OS revealed the presence of L-Rha, D-Glc, L,D-Hep, D,D-Hep, Kdo, Ko, D-GlcN and GlcN-*ol*. Methylation analysis revealed the presence of 3,4-substituted Hep, 2,7-substituted Hep, 3-substituted Hep, 7-substituted Hep, terminal L,D-Hep, terminal D,D-Hep, terminal D-Glc, terminal L-Rha, 6-substituted D-GlcN, 6-substituted D-GlcN-*ol*, 4,5-substituted D-Kdo, terminal D-Ko and, at very high retention time, a heptose disaccharide (Figure 1). A mild methanolysis treatment (0.5 M HCl/MeOH, 85 °C, 45 min), following the published method,[9] allowed the isolation of the trisaccharide Ara4N-(1→8)-Ko-(2→4)-Kdo.

A combination of homo- and heteronuclear 2D NMR experiments (DQF-COSY, TOCSY, ROESY, $^{13}$P-$^{1}$H HSQC, $^{13}$C-$^{1}$H HSQC and HMBC) was used to assign all the spin systems and the monosaccharide sequence. Several signals (**A**–**H**, Table 1) were identified in the anomeric region of the $^{1}$H NMR spectrum (Figure 2); furthermore, the signals at $\delta$ = 1.84/2.08 ppm were identified as the H-3 methylene of the Kdo residue. The anomeric configuration of each monosaccharide unit was assigned on the basis of the $^{3}J_{H1,H2}$ coupling constants obtained from the DQF-COSY experiment and the intraresidue NOE contacts observable in the ROESY spectrum, whereas the values of the vicinal $^{3}J_{H,H}$ coupling constants allowed the identification of each residue. The proton resonances of all spin systems were obtained by COSY and TOCSY (Figure 3) techniques and were used to assign the carbon resonances in the HSQC spectrum (Figure S1, Supporting Information). The NMR spectroscopic data indicated the existence of a complex mixture of oligosaccharides differing for the length of the carbohydrate backbone.

Due to the absence of anomeric proton signals, the reduced unit was assigned starting from the diastereotopic oxymethylene protons (residue **I**) resonating at $\delta$ = 3.46/3.63 ppm. The $^{13}$C-$^{1}$H HSQC spectrum shows a correlation

  

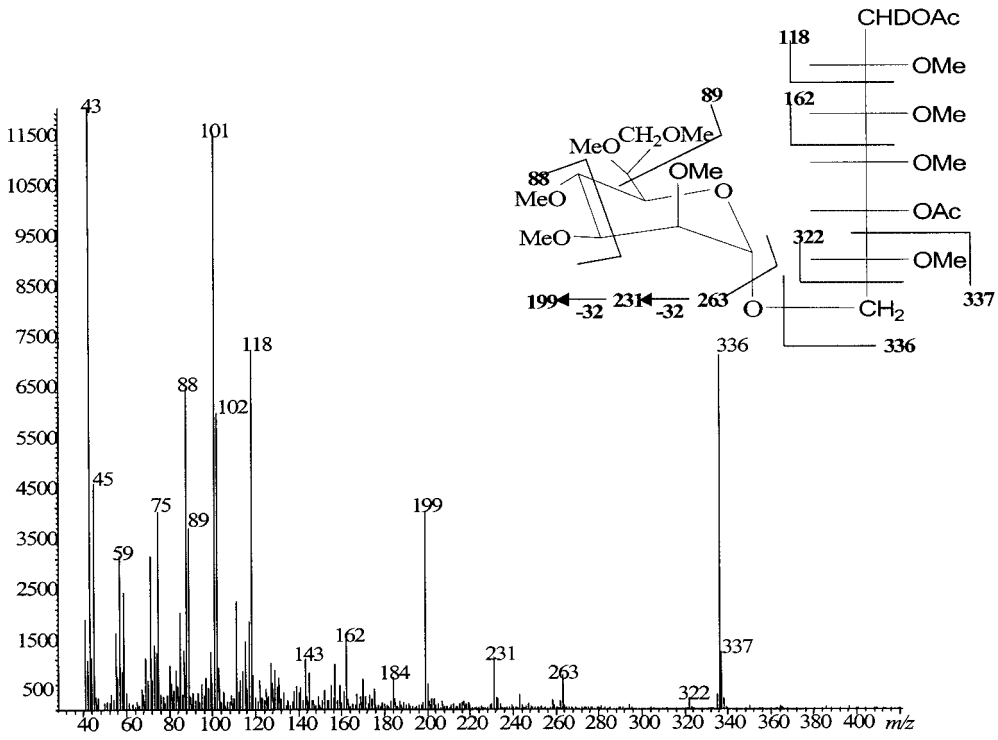


Figure 1. EI mass spectrum of the terminal D,D-Hep-(1→7)-α-L,D-Hep disaccharide of the core region of *B. pyrrocinia* isolated by methylation analysis; the structure and the main fragments are shown in the inset.

Table 1. $^{1}H$ and $^{13}C$ NMR chemical shifts (ppm) of sugar residues of the core-lipid A region of the oligosaccharide OS. The heptose residues, if not stated otherwise, possess an L-*glycero*-D-*manno* configuration. The ring coupling constant values are all in the range of 10 Hz, except for the *manno*-configured residues, in which the axial orientation gives low values (below 3 Hz); n.d.: not determined.

| Chemical shift $\delta$ ($^{1}H/^{13}C$) | | | | | | | | |
|---|---|---|---|---|---|---|---|---|
| Unit | 1 | 2 | 3 | 4 | 5 | 6 | 7 | 8 |
| **A** | 5.27 | 3.96 | 4.02 | 4.18 | 3.78 | 3.88 | 3.61 | |
| **3,4-α-Hep** | 99.1 | 71.5 | 75.5 | 72.61 | 70.0 | 69.7 | 62.7 | |
| **B** | 5.15 | 4.19 | 3.88 | 3.79 | 3.73 | 4.10 | 3.63 | |
| **2,7-α-Hep** | 99.6 | 74.1 | 69.7 | 70.2 | 70.5 | 67.9 | 69.5 | |
| **C** | 4.80 | 3.90 | 3.74 | 3.66 | 3.75 | 3.95 | 3.61/3.65 | |
| **t-α-Hep** | 100.1 | 69.8 | 70.5 | 67.2 | 70.5 | 68.9 | 63.0 | |
| **C′** | 4.83 | 3.90 | 4.16 | 3.96 | N.D. | n.d. | n.d. | |
| **3-α-Hep** | 100.6 | 69.6 | 77.4 | 68.9 | N.D. | n.d. | n.d. | |
| **D** | 4.93 | 3.93 | 3.79 | 3.60 | 3.74 | 3.93 | 3.60 | |
| **t-α-**D,D-Hep | 102.1 | 76.1 | 69.9 | 67.3 | 70.6 | 72.0 | 63.1 | |
| **E** | 4.98 | 4.03 | 3.75 | 3.66 | 3.82 | 3.94 | 3.61 | |
| **t-α-Hep** | 102.5 | 70.1 | 70.6 | 67.2 | 69.7 | 68.9 | 62.7 | |
| **E′** | 4.98 | 4.03 | 3.79 | 3.75 | 3.83 | 3.98 | 3.67 | |
| **7-α-Hep** | 102.4 | 72.2 | 70.0 | 70.8 | 72.3 | 68.5 | 69.7 | |
| **F** | 4.73 | 3.90 | 3.75 | 3.35 | 3.98 | 1.20 | | |
| **t-α-Rha** | 98.3 | 69.7 | 70.6 | 72.2 | 71.4 | 17.0 | | |
| **G** | 4.46 | 3.17 | 3.42 | 3.29 | 3.39 | 3.83/3.88 | | |
| **t-β-Glc** | 102.2 | 73.8 | 75.6 | 70.1 | 76.7 | 61.7 | | |
| **H** | 4.33 | 2.62 | 3.26 | 3.35 | 3.50 | 3.47/3.87 | | |
| **6-β-GlcNII** | 103.8 | 56.4 | 75.9 | 70.4 | 74.4 | 64.2 | | |
| **I** | 3.46/3.63 | 2.94 | 3.71 | 3.63 | 3.84 | 4.08/3.66 | | |
| **6-GlcN*ol*** | 62.9 | 53.7 | 69.8 | 71.7 | 69.8 | 71.8 | | |
| **K** | – | – | 1.84/2.08 | 4.09 | 4.13 | 3.66 | 3.95 | 3.68/3.82 |
| **4,5-α-Kdo** | 173.9 | 95.1 | 34.19 | 67.4 | 75.1 | 72.9 | 69.9 | 63.5 |
| **J** | – | – | 3.84 | 3.79 | 3.94 | 3.65 | 3.99 | 3.62/3.92 |
| **t-α-Ko** | 176.0 | 95.7 | 69.7 | 69.9 | 71.7 | 73.1 | 68.6 | 63.0 |

  

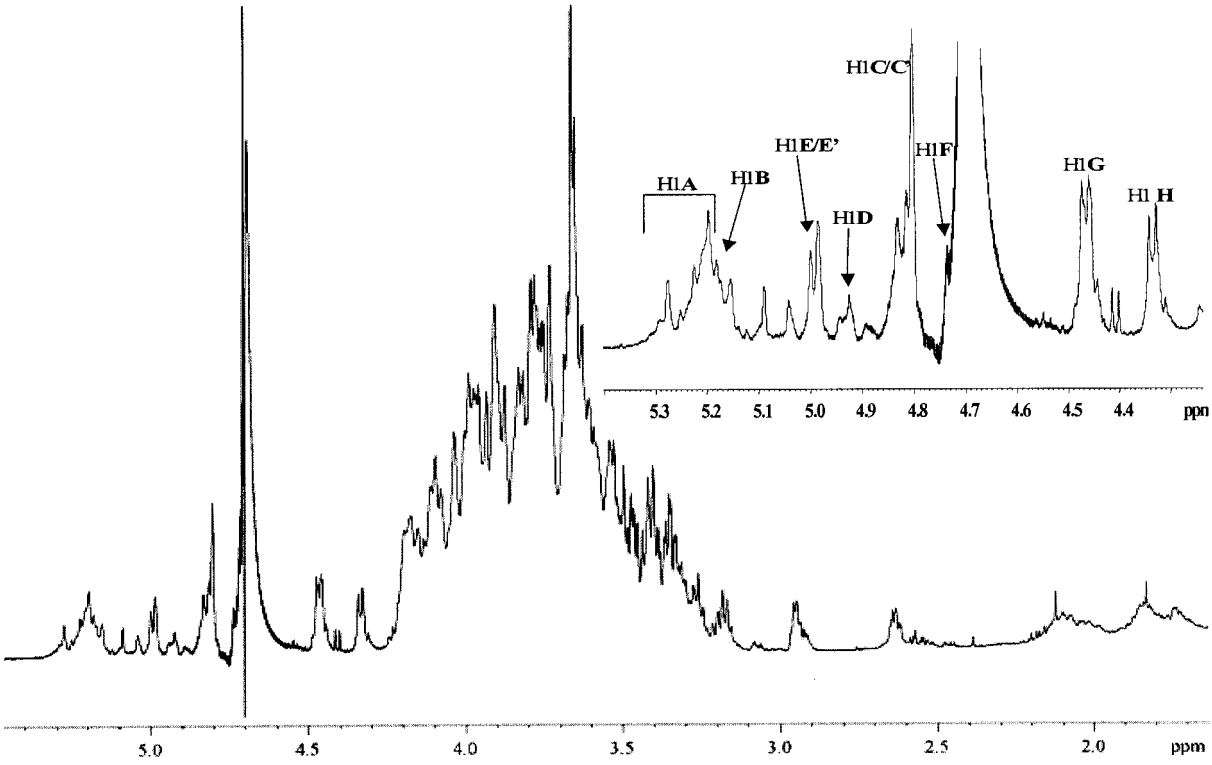


Figure 2. $^1$H NMR spectrum of product OS. The anomeric signals of the spin system are designated as in Table 1. Inset: the expanded anomeric region.

between H-2 **I**, at $\delta$ = 2.94 ppm, and a nitrogen-bearing carbon signal at $\delta$ = 53.7 ppm, which is diagnostic of a glucosaminitol residue (GlcN-*ol*), as expected from the GC-MS data. The anomeric signal of residue **H**, at $\delta$ = 4.33 ppm, is correlated in the HSQC spectrum to a carbon at $\delta$ = 103.8 ppm; this value, together with the $^3J_{H1,H2}$ coupling constant and the NOE contact of H-1 with H-3 and H-5 is diagnostic of a β-*gluco* configuration. The correlation of H-2 **H** with a high-field-shifted carbon signal at $\delta$ = 56.4 ppm is indicative of a C–N linkage at position 2. These data allowed us to define residue **H** as a β-GlcN unit. Hexose **G** possesses a β-*gluco* configuration, as determined by the vicinal $^3J_{H,H}$ coupling constant values and by the intraresidue NOE contacts of H-1 with H-3 and H-5.

Spin systems **A**, **B**, **C**, **C′**, **D**, **E** and **E′** (Table 1) were all identified as α-heptose residues, as indicated by their $^3J_{H1,H2}$ and $^3J_{H2,H3}$ coupling constants (below 3 Hz) and by the intraresidue NOE of H-1 with H-2. The $^{13}$C chemical shift value of C-6 of these heptoses allowed us to assign their diastereoisomeric nature. Thus, residues whose C-6 resonates below $\delta$ = 70 ppm were identified as L-*glycero*-D-*manno* heptose (**A**, **B**, **C**, **C′**, **E** and **E′**), whereas residue **D**, whose C-6 resonates at $\delta$ = 72 ppm, possesses a D-*glycero*-D-*manno* configuration.[10] Residue **F** (H-1 at $\delta$ = 4.73 ppm) was recognized as a α-rhamnose residue. In the TOCSY spectrum the scalar correlations of the ring protons with methyl signals resonating in the shielded region at $\delta$ = 1.20 ppm are visible. The *manno* configuration of residue **F** was established from the $^3J_{H1,H2}$ and $^3J_{H2,H3}$ values, the α-configuration by the intraresidue NOE contact of H-1 with H-2 and the chemical shift of its H-5 and C-5. Because of the absence of the anomeric proton signal, the spin system of Kdo (**K**) was assigned starting from the diastereotopic H-3 methylene protons, which resonate in a shielded region at $\delta$ = 1.84 and 2.08 ppm (H-3$_{ax}$ and H-3$_{eq}$, respectively). The α-configuration at C-2 was attributed from the chemical shift values of H-3 and the values of the $^3J_{H7,H8a}$ and $^3J_{H7,H8b}$[11,12] coupling constants. Residue **J** of α-Ko was assigned starting from its carbinolic H-3 signal group, which resonates at $\delta$ = 3.84 ppm. The relative and anomeric configurations of the ring were assigned by analysis of the vicinal $^3J_{H,H}$ coupling constants from the DQF-COSY spectrum and comparison with published data.[9] The downfield shift of the carbon resonances identified the glycosylated positions: O-6 of residues **H** and **I**, O-3 of **C′**, O-7 of **E′**, O-4 and O-5 of **K**, O-3 and O-4 of **A** and O-2 and O-7 of **B**, whereas residues **C**, **D**, **E**, **F**, **G** and **J** were found to be non-reducing terminal sugars, in full agreement with the methylation analysis data. The inter-residue NOE contacts (Figure 3) and the long-range correlations present in the HMBC spectrum yielded the sequence of monosaccharides (see Figure S2 in the Supporting Information).

The inter-residue NOE contact of H-1 of **H** ($\delta$ = 4.33 ppm) with H-6$_{a,b}$ of **I** ($\delta$ = 4.08/3.66 ppm), together with the downfield shift of C-6 of **I**, validated the β-(1→6) linkage between β-GlcN (**H**) and GlcN-*ol* (**I**) of the lipid A backbone. Due to the absence of the anomeric proton of Kdo (**K**), its linkage to β-GlcN (**H**) could be established by the downfield $^{13}$C chemical shift of C-6 of **H** ($\delta$ = 64.2 ppm, Table 1) and by the long-range correlation in the HMBC

  

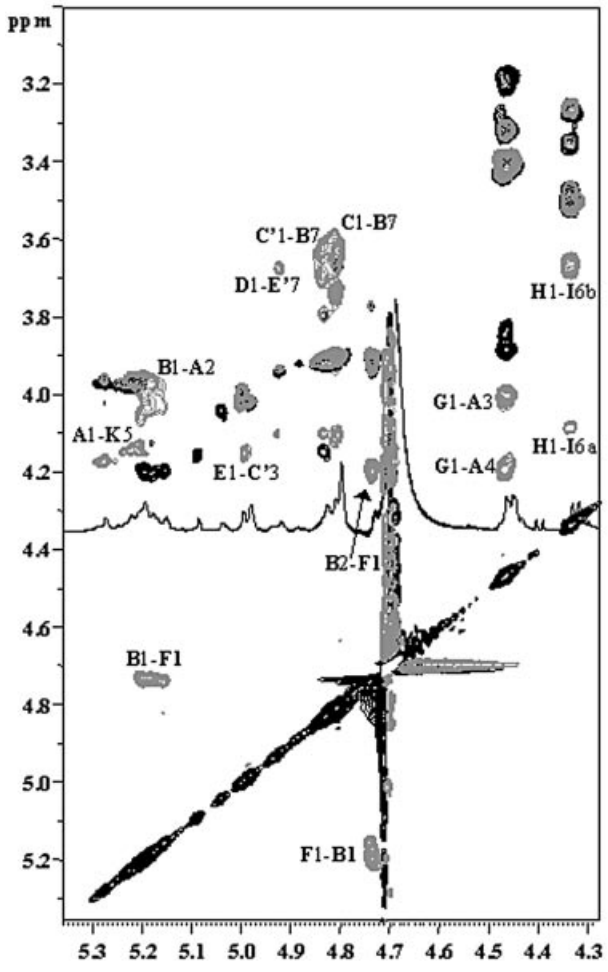


Figure 3. Section of the ROESY (grey) and TOCSY (black) spectrum of oligosaccharide OS. Monosaccharide labels are as indicated in Table 1. The relevant inter-residue ROE cross-peaks are indicated.

spectrum between C-2 of **K** and H-6 of **H**, all of which are diagnostic of the α-(2→6) ketosidic linkage of Kdo (**K**) with residue **H** of β-GlcN. The Kdo residue **K** was found to be glycosylated at both positions 4 and 5. The long-range correlation in the HMBC spectrum between C-2 of **J** ($\delta$ = 95.7 ppm) and H-4 of **K** ($\delta$ = 4.09 ppm) is diagnostic of an α-(2→4) ketosidic linkage to Ko (**J**). The NOE contact between H-1 of **A** ($\delta$ = 5.27 ppm) and H-5 and H-7 of **K** ($\delta$ = 4.13 and 3.95 ppm, respectively; Figure 3) indicates the α-(1→5) linkage of α-Hep (**A**) to Kdo (**K**). Moreover, these NOE contacts also provide further information regarding the absolute configuration of Kdo (**K**) as they are compatible only with the D-configuration.[12] Residue **A** is, in turn, substituted at O-3 and O-4. The NOE contact between H-4 of **A** ($\delta$ = 4.18 ppm) and H-1 of **G** ($\delta$ = 4.46 ppm) suggests that the O-4 of α-heptose **A** is glycosylated by residue **G** of β-glucose. Residue **A** is also substituted at O-3 by residue **B**, according to the NOE (Figure 3) between H-3 of **A** ($\delta$ = 4.02 ppm) and H-1 of **B** ($\delta$ = 5.15 ppm). Residue **B** was identified as a 2,7-disubstituted α-heptose. The NOE correlation between H-2 of **B** ($\delta$ = 4.19 ppm) and H-1 of **F** ($\delta$ = 4.73 ppm) (Figure 3) provides evidence for substitution of residue **B** at O-2 by α-rhamnose **F**. Furthermore, residue **B** is glycosylated at O-7 by the heptose residue **C**, as demonstrated by the NOE contact between H-7 of **B** and H-1 of **C**.

The methylation analyses, glycosylation shifts and NOE data are all in agreement with the oligosaccharide structure reported below (oligosaccharide **X**).

**C**-(1→7)-**B**-(1→3)-**A**-(1→5)-**K**-(2→6)-**H**-(1→6)-**I**
2 4 4
↑ ↑ ↑
1 1 2
**F** **G** **J**

The HMBC spectrum confirms the structure assigned so far since it contains all the required long-range correlations to demonstrate the proximity of the residues (Figure S2).

An alternative spin system was identified for residue **C**, namely 3-substituted heptose, indicated as residue **C′** (Table 1 and Figures 2 and 3). This residue is substituted at O-3 by the terminal heptose **E**, as shown by the NOE contact between H-3 of **C′** ($\delta$ = 4.16 ppm) and H-1 of **E** ($\delta$ = 4.98 ppm), thus validating the following structure (oligosaccharide **Y**).

**E**-(1→3)- **C'**-(1→7)-**B**-(1→3)-**A**-(1→5)-**K**-(2→6)-**H**-(1→6)-**I**
2 4 4
↑ ↑ ↑
1 1 2
**F** **G** **J**

Residue **E** is, in turn, non-stoichiometrically substituted at O-7, as shown by the discovery of the alternative glycoform **E′**, which is a 7-substituted heptose. The NOE contact between H-7 of **E′** and H-1 of the D,D-heptose residue **D** helped us to identify the oligosaccharide **Z**, where a terminal α-(1–7) heptose disaccharide, as found also by methylation analysis (see above and Figure 1), is present.

**D**-(1→7)-**E'**-(1→3)- **C'**-(1→7)-**B**-(1→3)-**A**-(1→5)-**K**-(2→6)-**H**-(1→6)-**I**
2 4 4
↑ ↑ ↑
1 1 2
**F** **G** **J**

The OS sample was also subjected to ESI mass spectrometric analysis. The positive-ion mass spectrum (Figure 4) shows three groups of peaks, all doubly charged, indicative of a mixture of oligosaccharides. The ions at *m*/*z* 1043.0 and 1035.0, corresponding to $[M + H + NH_4]^+/2$ and $[M + 2H]^+/2$, respectively, are consistent with the undecasaccharide **Z**. The decasaccharide **Y**, which differs from sample **Z** by a heptose unit, is represented by the ions at *m*/*z* 947.1 and 938.6, which correspond to $[M + H + NH_4]^+/2$ and $[M + 2H]^+/2$, respectively. The nonasaccharide **X**, which lacks a second heptose residue, is consistent with the peak at *m*/*z* 850.9 $[M + H + NH_4]^+/2$. These data are in full agreement with the structural hypotheses obtained from NMR experiments.

A MALDI mass spectrum of the oligosaccharide mixture (Figure S3 in the Supporting Information) completely confirmed the above structural hypotheses. The negative-ion mass spectrum shows three major ions at *m*/*z* 2066.3, 1874.2

  

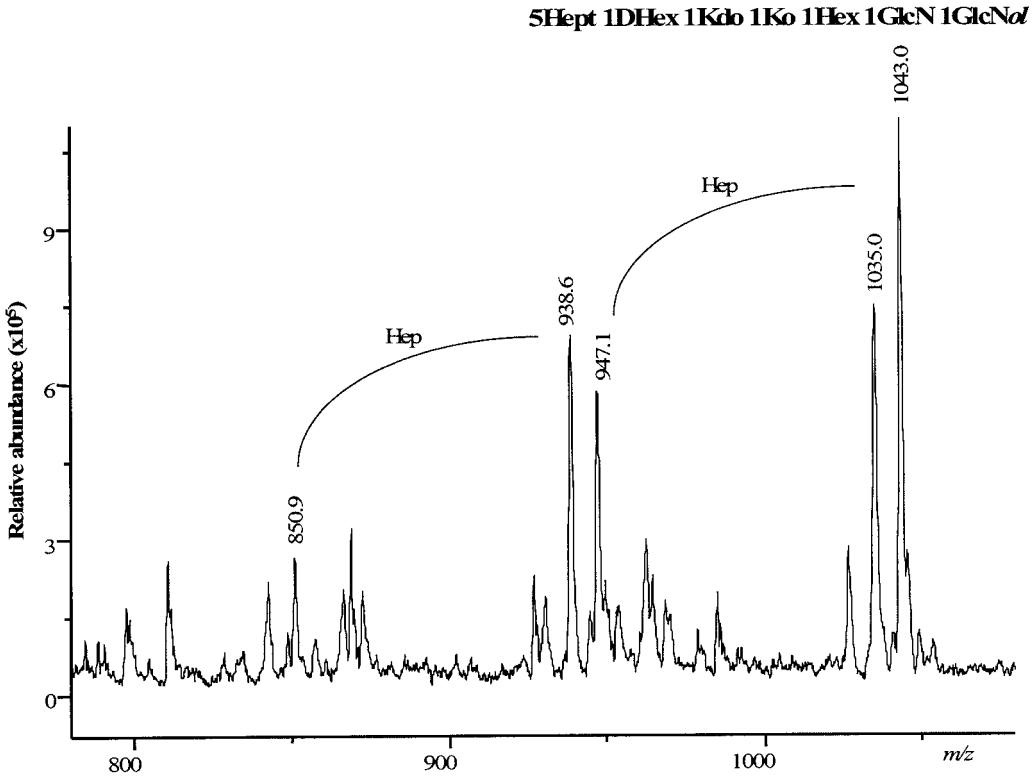


Figure 4. Positive-ion ESI mass spectrum of OS product. Assignment of the ion peaks is shown.

and 1681.6 ($\Delta m/z$ = 192). The species at *m*/*z* 2066.3 was identified as the undecasaccharide **Z**, built up of five Hep, one deoxy-Hex, one Kdo, one Ko, one Hex, one HexN and one HexN*ol* residues. The species at *m*/*z* 1874.2 ($\Delta m/z$ 192) is consistent with the decasaccharide **Y**, which differs from **Z** by the absence of one heptose residue. Finally, the ion at *m*/*z* 1681.6 was identified as the nonasaccharide **X**, which lacks a second heptose unit.

## Structural Characterisation of the Intact LOS Molecule

In order to confirm the structure of the lipid A-core region and gain more information on the non-carbohydrate substituents, the intact LOS was analysed by MALDI mass spectrometry. The negative-ion mass spectrum (Figure 5 and Figure S4 in the Supporting Information) shows, besides the molecular ions in the mass range 3000–4000 Da,

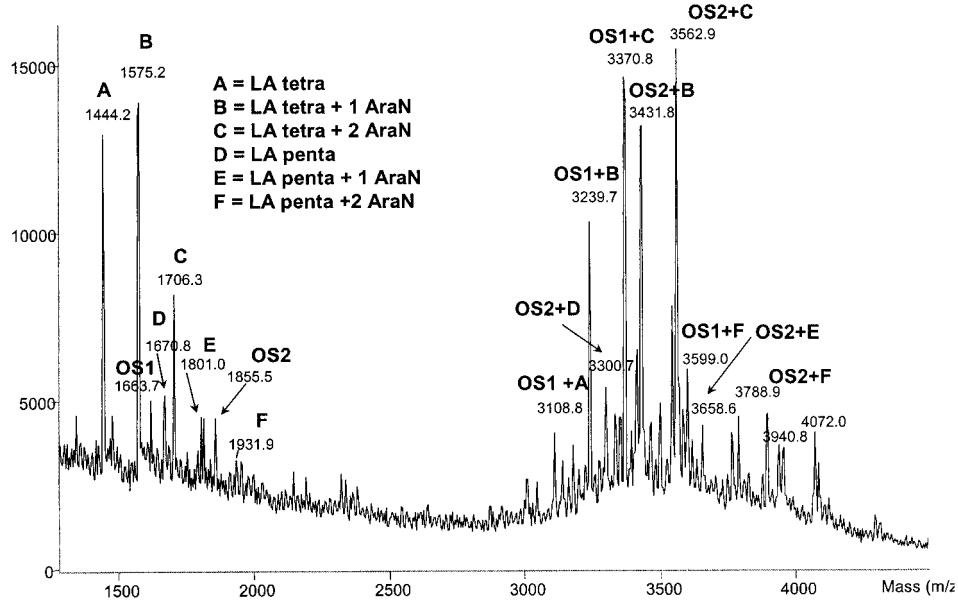


Figure 5. Negative-ion MALDI TOF mass spectrum of the intact LOS of *B. pyrrocinia* obtained in linear mode at high laser intensity.

  

peaks related to fragments arising from the very labile glycosidic bond cleavage between Kdo and the lipid A moiety.[13] This fragmentation arises from a β-elimination and yields either an oligosaccharide ion (B-type fragments), or a lipid A ion.

The lipid A (LA in the figure text) is made up from a heterogeneous mixture of tetra- and penta-acylated species that differ in the phosphorylation pattern (species **A**–**F**) (Figures 5 and S5 in the Supporting Information). Species **A**, at *m*/*z* 1444.2, is consistent with a tetra-acylated disaccharide backbone carrying one 14:0 (3-OH) chain in an ester linkage and two 16:0 (3-OH) chains in an amide linkage, one of which − that on the GlcN II − is further substituted by a secondary fatty acid (a 14:0 residue); species **B**, at *m*/*z* 1575.2 (Δ*m*/*z* = 131), carries an Ara4N residue. Species **D** and **E** are the corresponding penta-acylated species carrying two ester-linked 14:0 (3-OH) residues, while species **C** and **F** are tetra- and penta-acylated species substituted by two phosphoryl arabinosamine residues. The lipid A structure is not discussed in detail because it is in full accordance with that previously determined.[8] A series of ions present in the same mass range (Figures 5 and S5 in the Supporting Information) are derived from the core oligosaccharide and are in accordance with the above structural description. The ion peak at *m*/*z* 1855.5 (OS2) corresponds to a decasaccharide carrying five heptoses, one deoxyhexose, one hexose, one Kdo, one Ko and one pentosamine, which was identified by GC-MS as Ara4N. This latter residue is obviously linked at position O-8 of the Ko residue, as shown by the GC-MS analysis, which shows the existence of a Kdo-Ko-Ara4N trisaccharide, in accordance with previously published data.[9,14,15] The glycosidic linkage of the Ara4N unit is most likely cleaved during the HF treatment performed to remove the phosphate groups, thus explaining its absence

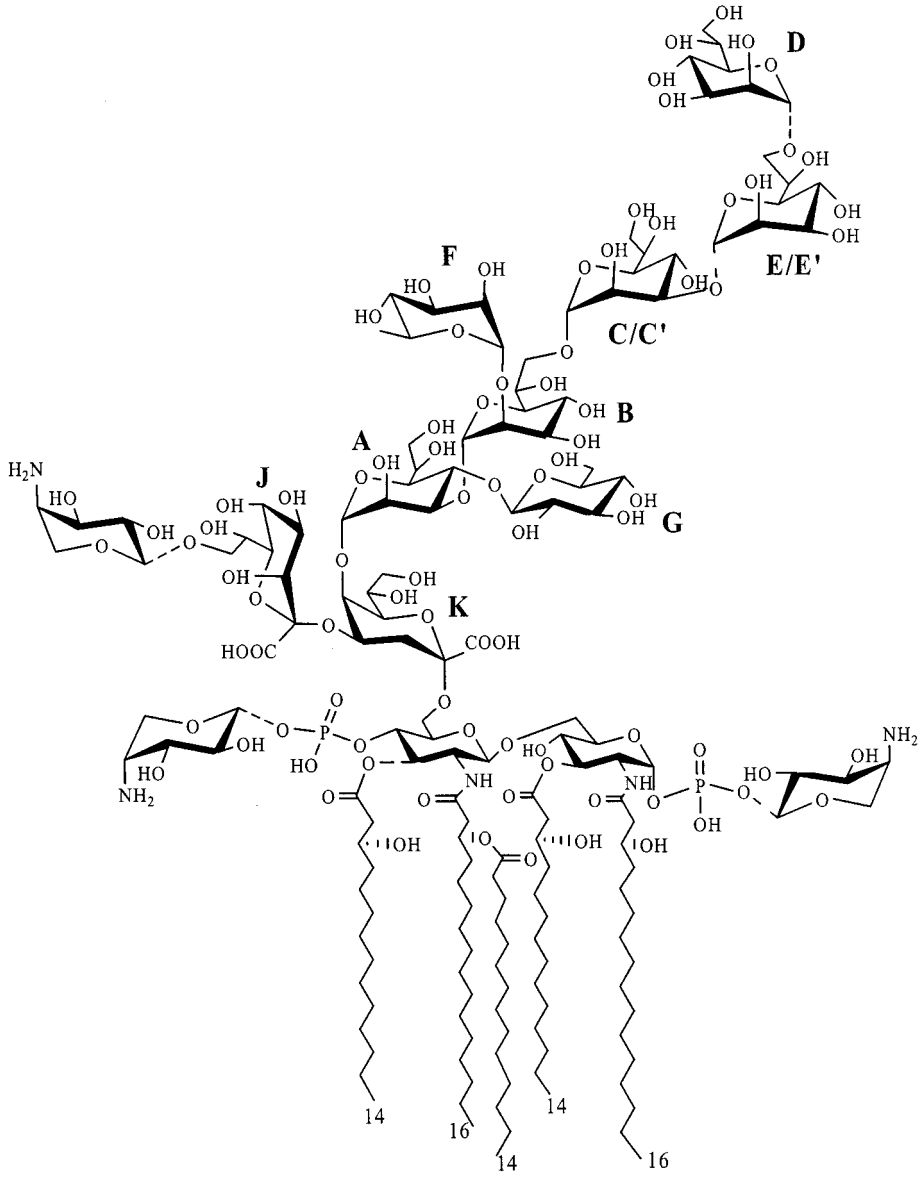


Figure 6. The structure of the lipooligosaccharide from *Burkholderia pyrrocinia*. The dotted lines indicate non-stoichiometric substitution.

  

from the deacylated and reduced oligosaccharide analysed previously. In summary, ion OS2 is the core fragment of intact LOS that chemically matches the oligosaccharide **Z**, without the lipid A part but containing an Ara4N unit linked to the Ko residue. Analogously, the OS1 ion (*m*/*z* 1663.8) differs from OS2 only by the lack of a heptose residue (Δ*m*/*z* 192) and chemically matches the oligosaccharide **Y**. The core fragment corresponding to oligosaccharide **X** was not detectable in the MALDI mass spectrum. All peaks described above originate from a β-elimination of the molecular ions that can clearly be determined by the addition of the fragment ions. In summary, the complete structure of the lipooligosaccharide (Figure 6) from the clinical isolate of *Burkholderia pyrrocinia* strain BTS7 has been carried out by chemical analyses, MALDI and ESI mass spectrometry and 2D NMR spectroscopy.

## Discussion

Recurrent and chronic respiratory tract infections in patients with CF might result in progressive lung damage and subsequently lead to death. Infections are usually caused by *Pseudomonas aeruginosa*, *Staphylococcus aureus*, *Haemophilus influenzae* and species of the *Burkholderia cepacia* complex. The latter are problematic CF pathogens because they are very resistant to antibiotics, cause infection associated with high mortality in CF, are responsible for patient-to-patient transmission and are difficult to identify. To date, the BCC includes nine distinct species[2] that differ in their virulence potential, and among the virulence factors of the BCC, a central role might be ascribed to the LPS.[16] The LPS toxicity is well known, but only a relatively small amount of data are available on the primary structure of the LPS components produced by species of the BCC, especially on the clinical isolates.

*B. pyrrocinia* strain BTS7, a highly mucoid strain, was isolated from a CF patient. In free-living culture, *B. pyrrocinia* only expresses the R-form LPS, namely a lipooligosaccharide (LOS) that, for the first time, has been purified and completely identified by chemical analysis, NMR spectroscopy and mass spectrometry.

The lipooligosaccharide (Figure 6) is built up of a heterogeneous lipid A consisting of several differently acylated and glycosylated chemical species and a core oligosaccharide whose carbohydrate backbone varies in length due to monose residues present in non-stoichiometric amounts. The fatty acid and polar heads composition and substitution in lipid A completely resemble the analogous ones found in other *Burkholderia*.[15,17]

The conversion to the mucoid state in *P. aeruginosa*, another important pathogen of CF patients, is often associated with loss of O-chain production,[18–20] which usually renders the bacteria serum resistant. At the same time, alginate, the exopolysaccharide produced by this species, is *O*-acetylated, a characteristic that maximises the resistance of these bacteria to antibody-independent phagocytic killing.[21] Likewise, *B. pyrrocinia* BTS7 is a mucoid isolate that produces abundant quantities of an exopolysaccharide named cepacian, which is *O*-acetylated and possesses macromolecular and solution properties similar to those of bacterial alginate.[22] In the same way, *B. pyrrocinia* only produces O-chain-lacking lipopolysaccharides (LOS). Thus, the lack of the O-chain in the LPS of this mucoid strain and the similar molecular properties exhibited by the two exopolysaccharides cepacian and alginate are interesting features that suggest that the two bacterial species *P. aeruginosa* and *B. pyrrocinia* might share common strategies to elude the host immune defences.

The lipid A moiety, as previously determined,[8] possesses a carbohydrate backbone characterised by a [P→4-β-D-Glc*p*N-(1→6)-α-D-Glc*p*N-1→P] sequence and is further glycosylated by a Kdo unit that is, in turn, substituted at O-5 with a Ko residue. The latter might bear an Ara4N residue. The Ara4N→Ko→Kdo trisaccharide, previously known from other *Burkholderia* species,[9,14,15] unequivocally characterised in this work by GC-MS and MALDI analyses, seems to be a peculiarity of all *Burkholderia* LPSs. The Ko monosaccharide is rather rare and is present only in a few other bacterial LPSs, like *Acinetobacter*[23] and *Yersinia*.[24]

The Kdo unit is substituted at O-5 by the pentasaccharide α-L,D-Hep-(1→7)-[α-L-Rha-(1→2)]-α-L,D-Hep-(1→3)-[β-D-Glc-(1→4)]-α-L,D-Hep-(1→, which is common to the LOSs found in *B. cepacia*.[14] The heptose residue of this pentasaccharide portion can be further substituted at O-7 by another heptose residue that carries an α-D,D-Hep-(1→7)-α-L,D-Hep-(1→ disaccharide at O-3.

The lipooligosaccharide biosynthesis can strongly be influenced by the physiological environment. Under stress conditions, LPS can modify its primary structure to reinforce the external membrane and to assure the bacteria an adequate protection. A characteristic of species belonging to the *B. cepacia* complex is their resistance to antimicrobial cationic peptides, which are released by a variety of organisms, including mammals and plants, and which, in humans, are part of the innate immune response to bacterial infections. These peptides damage and definitively kill microorganisms by inserting into their membrane and forming pores.[25] Transmembrane pore formation is possibly not the only mechanism of microbial killing, since translocated peptides can alter cytoplasmic membrane septum formation and inhibit cell wall, nucleic acids, and proteins synthesis or enzymatic activity. Bacteria can adopt several mechanisms to increase the resistance to antimicrobial peptides, all of which involve structural changes in their outer and inner membranes, i.e. modifications that are able to assure chemical protection, including the alteration of the net surface charge. The electrostatic interactions on the surface of the external membrane are, in fact, believed to contribute to reducing the membrane permeability and enhancing its stability by forming a strong, rigid and protective barrier. Positively charged substituents present in the lipid A-core region (Ara4N, EtN) can substitute divalent cations in the interaction with negatively charged groups on the external surface. Consequently, the entrance of positively charged

  

macromolecules such as antibacterial cationic peptides and antibiotics is hindered.

In coherence with the above hypotheses, the LOS of *B. pyrrocinia* not only lacks the typical negatively charged substituents in the inner core region but also carries 4-amino-4-deoxyarabinose (Ara4N), a cationic substituent that confers antimicrobial peptide resistance[25,26] by reducing the entrance of positively charged macromolecules due to a decreased net surface charge. Recently, it has been demonstrated that while the resistance to antimicrobial peptides requires the lipid A-inner core region,[26] which seems to be indispensable for bacterial survival in vivo, the lack of the O-antigen does not impair bacterial resistance, thereby leading to the conclusion that this portion is not responsible for sensitivity to antimicrobials.

The understanding of how different LPS chemical structures determine changes in the pathogenic potential of the BCC infection is, in our opinion, a mandatory step to define the relationship between LPS structure and toxicity and to develop novel therapeutic strategies.

## Experimental Section

**Bacterial growth and LPS extraction:** *B. pyrrocinia* BTS7[7] was isolated from a CF patient attending the Regional Centre for Cystic Fibrosis, Children's Hospital Burlo Garofolo, Trieste. The bacteria were cultivated in liquid Luria Bertani medium enriched with 0.2% glucose for 3 d at 30 °C with shaking. The culture broth was then centrifuged and the cells were washed with 0.5% NaCl and freeze-dried.

The dried cells (4.8 g) were extracted with chloroform/light petroleum/phenol according to the conventional procedures.[27,28] Dried cells were extracted three times with a mixture of 2:5:8 aqueous 90% phenol/chloroform/light petroleum (v/v/v) as described. To get rid of all the cell contaminants, the LPS fraction was further subjected to enzymatic hydrolysis with RNase, DNase, and proteinase K followed by size-exclusion chromatography on Sephacryl S-300 in 50 mM $NH_4CO_3$ (yield 170 mg, 1.5% of dried cells). Sodium dodecyl sulfate polyacrylamide gel electrophoresis (SDS-PAGE 12%) was performed as described previously; gels were stained with silver nitrate for detection of LPS and LOS.[28,29]

**Isolation of OS:** An aliquot of LOS (20 mg) was dissolved in anhydrous hydrazine (2 mL), stirred at 37 °C for 90 min, cooled, poured into ice-cold acetone (20 mL), and allowed to precipitate. The precipitate was then centrifuged (3000 g, 30 min), washed twice with ice-cold acetone, dried, dissolved in water and lyophilised. The sample was subsequently treated with 48% aqueous HF (4 °C, 48 h) to remove phosphate groups and then reduced with $NaBH_4$ (room temp., 18 h) and de-*N*-acylated with 4 M KOH. After desalting on a column (50 × 1.5 cm) of Sephadex G-10 (Pharmacia), the resulting oligosaccharide fraction (5 mg) was further purified by gel-permeation chromatography on Bio-Gel P6 (Pharmacia) in water.

**General and Analytical Methods:** Determination of sugar residues, including the determination of the absolute configuration, organic-bound phosphate, and the absolute configuration of the hexoses were all carried out as described elsewhere.[30–33] For methylation analysis of the Kdo region, LOS was carboxymethylated with methanolic HCl (0.1 M, 5 min) and then with diazomethane to improve its solubility in $Me_2SO$. Methylation was carried out as described previously.[34,35] LOS was hydrolysed with 2 M trifluoroacetic acid (100 °C, 1 h), carbonyl-reduced with $NaBD_4$, carboxymethylated as described above, carboxyl-reduced with $NaBD_4$ (4 °C, 18 h), acetylated and analysed by GLC-MS.

Total fatty acid content was obtained as described previously.[8]

**NMR Spectroscopy:** For structural assignments of OS, 1D and 2D $^1$H NMR spectra were recorded with a solution of 2 mg of sample in 0.5 mL of $D_2O$ at 300 K and pD 7 with a Bruker 600 DRX spectrometer equipped with a cryo probe. Spectra were calibrated against internal acetone ($\delta_H$ = 2.225, $\delta_C$ = 31.45 ppm).

Rotating frame Overhauser enhancement spectroscopy (ROESY) was measured using data sets ($t_1 \times t_2$) of 4096 × 256 points with a mixing time of 200 ms. Double quantum-filtered phase-sensitive COSY experiments were performed with a 0.258-s acquisition time, using data sets of 4096 × 256 points. Total correlation spectroscopy experiments (TOCSY) were performed with a spinlock time of 100 ms, using data sets ($t_1 \times t_2$) of 4096 × 256 points. In all homonuclear experiments the data matrix was zero-filled in the *F*1 dimension to give a matrix of 4096 × 2048 points and was resolution-enhanced in both dimensions by a sine-bell function before Fourier transformation. Coupling constants were determined on a first-order basis by 2D phase-sensitive double-quantum-filtered correlation spectroscopy (DQF-COSY).[36,37] Heteronuclear single quantum coherence (HSQC) and heteronuclear multiple bond correlation (HMBC) experiments were measured in the $^1$H-detected mode by single quantum coherence with proton decoupling in the $^{13}$C domain, using data sets of 2048 × 256 points. Experiments were carried out in the phase-sensitive mode. A 60-ms delay was used for the evolution of long-range connectivities in the HMBC experiment. In all heteronuclear experiments the data matrix was extended to 2048 × 1024 points using forward linear prediction extrapolation.[38,39]

**MALDI TOF and ESI Analyses:** ESI mass spectra were recorded with an API-I PE SCIEX quadrupole mass spectrometer equipped with an articulated ion spray connected to a syringe pump for the injection of the samples. The instrument was calibrated using a polypropylene glycol mixture ($3.3 \times 10^{-5}$ M polypropylene glycol $M_n$ = 425/$1 \times 10^{-4}$ M polypropylene glycol $M_n$ = 1000/$2 \times 10^{-4}$ M polypropylene glycol $M_n$ = 2000), 0.1% acetonitrile and 2 mM ammonium formate in 50% aqueous methanol.

The OS sample was desalted on a Bio-Gel P-2 column, converted to its ammonium salt form[40] and dissolved in 50% aqueous acetonitrile/$0.13 \times 10^{-3}$ M ammonium acetate. The spectra were recorded in the positive-ion mode, using an injection flow rate of 5 μL min$^{-1}$, with the ion-spray voltage at 5000 V and the orifice potential at 50 V, and using a step size of 0.1 amu.

MALDI-TOF analyses were conducted in linear mode using a Perseptive (Framingham, MA, USA) Voyager STR instrument equipped with delayed extraction technology. Ions formed by a pulsed UV laser beam (nitrogen laser, $\lambda$ = 337 nm) were accelerated through 24 kV. Mass spectra reported are the result of 256 laser shots. Sample preparation was performed adopting our "LOS thin-layer procedure" as described previously.[13] Briefly, both the OS species and the intact LOS were first converted in the ammonium form on a cation-exchanged resin Dowex 50WX8-200 (Sigma–Aldrich). The obtained samples were then deposited on the top of a thin layer of 2,4,6-trihydroxyacetophenone (THAP)/nitrocellulose matrix together with the same volume of 20 mM dibasic diammonium citrate.

**Supporting Information** (see also the footnote on the first page of this article): DEPT-HSQC and HMBC spectra and the MALDI

  

mass spectrum of the oligosaccharide OS, zoomed part of the MALDI mass spectrum of the intact LOS.

## Acknowledgments

NMR facilities were provided by the Centro Regionale di Competenza in Biotecnologie Industriali BioTekNet. This work was financially supported (M.P.) by MIUR-Roma (Progetto di Ricerca di Interesse Nazionale, 2004, Roma).

[1] J. R. W. Govan, V. Deretic, *Microbiol. Rev.* **1996**, *60*, 539–574.
[2] K. Vermis, T. Coenye, E. Mahenthiralingam, H. J. Nelis, P. Vandamme, *J. Med. Microbiol.* **2002**, *51*, 937–940.
[3] G. Seltmann, O. Holst, *The Bacterial Cell Wall*, Springer, Heidelberg, **2001**.
[4] O. Holst, in *Endotoxins in Health and Disease* (Eds.: H. Brade, D. C. Morrsion, S. Opal, S. Vogel), Marcel Dekker, New York, **1999**, pp. 115–154.
[5] C. Alexander, E. T. Rietschel, *J. Endotoxin Res.* **2001**, *7*, 167–199.
[6] O. Holst, *Trends Glycosci. Glycotechnol.* **2002**, *14*, 87–103.
[7] C. Lagatolla, S. Skerlavaj, L. Dolzani, E. A. Tonin, C. Monti Bragadin, M. Bosco, R. Rizzo, L. Giglio, P. Cescutti, *FEMS Microbiol. Lett.* **2002**, *209*, 99–106.
[8] A. Silipo, A. Molinaro, P. Cescutti, E. Bedini, R. Rizzo, M. Parrilli, R. Lanzetta, *Glycobiology* **2005**, *15*, 561–570.
[9] Y. Isshiki, K. Kawahara, U. Zahringer, *Carbohydr. Res.* **1998**, *313*, 21–27.
[10] A. Silipo, S. Leone, A. Molinaro, L. Sturiale, D. Garozzo, E. L. Nazarenko, R. P. Gorshkova, E. P. Ivanova, R. Lanzetta, M. Parrilli, *Eur. J. Org. Chem.* **2005**, 2281–2291.
[11] G. I. Birnbaum, R. Roy, J. R. Brisson, H. Jennings, *J. Carbohydr. Chem.* **1987**, *6*, 17–39.
[12] O. Holst, J. E. Thomas-Oates, H. Brade, *Eur. J. Biochem.* **1994**, *222*, 183–194.
[13] L. Sturiale, D. Garozzo, A. Silipo, R. Lanzetta, M. Parrilli, A. Molinaro, *Rapid Commun. Mass Spectrom.* **2005**, *19*, 1829–1834.
[14] I. Isshiki, U. Zahringer, K. Kawahara, *Carbohydr. Res.* **2003**, *338*, 265.
[15] S. Gronow, C. Noah, A. Blumenthal, B. Lindner, H. Brade, *J. Biol. Chem.* **2003**, *278*, 1647–1655.
[16] S. M. Zughaier, H. C. Ryley, S. K. Jackson, *Infect. Immun.* **1999**, *67*, 1505–1507.
[17] A. Molinaro, C. De Castro, R. Lanzetta, A. Evidente, M. Parrilli, O. Holst, *J. Biol. Chem.* **2002**, *277*, 10058–10063.
[18] R. E. W. Hancock, L. M. Nutharia, L. Chan, R. P. Darveau, D. P. Speert, G. B. Pier, *Infect. Immun.* **1983**, *42*, 170–177.
[19] B. Ojeniyi, L. Baek, N. Hoiby, *Acta Pathol. Microbiol. Immunol. Scand.* **1985**, *93*, 7–13.
[20] A. Penketh, T. Pitt, D. Roberts, M. E. Hodson, J. C. Batten, *Am. Rev. Respir. Dis.* **1983**, *127*, 605–608.
[21] G. B. Pier, F. Coleman, M. Grout, M. Franklin, D. E. Ohman, *Infect. Immun.* **2001**, *69*, 1895–1901.
[22] P. Sist, P. Cescutti, S. Skerlavaj, R. Urbani, J. H. Leitão, I. Sá-Correia, R. Rizzo, *Carbohydr. Res.* **2003**, *338*, 1861–1867.
[23] E. V. Vinogradov, K. Bock, B. O. Petersen, O. Holst, H. Brade, *Eur. J. Biochem.* **1997**, *243*, 122–127.
[24] E. V. Vinogradov, B. Lindner, N. A. Kocharova, S. N. Senchenkova, A. S. Shashkov, Y. A. Knirel, O. Holst, T. A. Gremyakova, R. Z. Shaikhutdinova, A. P. Anisimov, *Carbohydr. Res.* **2002**, *337*, 775–777.
[25] K. A. Brogden, *Nat. Rev. Microbiol.* **2005**, *3*, 238–250 and references cited therein.
[26] S. A. Loutet, R. S. Flannagan, C. Kooi, P. A. Sokol, M. A. Valvano, *J. Bacteriol.* **2006**, *188*, 2073–2080 and references cited therein.
[27] C. Galanos, O. Lüderitz, O. Westphal, *Eur. J. Biochem.* **1969**, *9*, 245–249.
[28] O. Westphal, K. Jann, *Meth. Carbohydr. Chem.* **1965**, *5*, 83–91.
[29] R. Kittelberger, F. Hilbink, *J. Biochem. Biophys. Methods* **1993**, *26*, 81–86.
[30] O. Holst, in *Methods in Molecular Biology, Bacterial Toxins: Methods and Protocols* (Ed.: O. Holst), Humana Press Inc, Totowa, NJ, **2000**, pp. 345–353.
[31] E. Vinogradov, A. Korenevsky, T. J. Beveridge, *Carbohydr. Res.* **2003**, *338*, 1991–1997.
[32] E. Vinogradov, A. Korenevsky, T. J. Beveridge, *Carbohydr. Res.* **2004**, *339*, 737–740.
[33] E. Vinogradov, K. Bock, B. O. Petersen, O. Holst, H. Brade, *Eur. J. Biochem.* **1997**, *243*, 122–127.
[34] I. Ciucanu, F. Kerek, *Carbohydr. Res.* **1984**, *131*, 209–217.
[35] S. Hakomori, *J. Biochem. (Tokyo)* **1964**, *55*, 205–208.
[36] U. Piantini, O. W. Sørensen, R. R. Ernst, *J. Am. Chem. Soc.* **1982**, *104*, 6800–6801.
[37] M. Rance, O. W. Sørensen, G. Bodenhausen, G. Wagner, R. R. Ernst, K. Wüthrich, *Biochem. Biophys. Res. Commun.* **1983**, *117*, 479–485.
[38] R. de Beer, D. van Ormondt, *NMR Basic Principles and Progress* (Ed.: M. Rudin), vol. 26, Springer, Berlin, **1992**, p. 201.
[39] J. C. Hoch, A. S. Stern, *NMR Data Processing* (Eds.: J. C. Hoch, A. S. Stern), John Wiley & Sons, New York, **1996**, pp. 77–101.
[40] R. Korner, G. Limberg, J. D. Mikkelsen, P. Roepstorff, *J. Mass Spectrom.* **1998**, *33*, 836–842.

Received: June 15, 2006
Published Online: September 7, 2006

  